Electronic transport in ultrathin magnetic multilayers

J. Barnaś* and Y. Bruynseraede
Laboratorium voor Vaste-Stoffysika en Magnetisme, Katholieke Universiteit Leuven, Celestijnenlaan 200 D, B-3001 Leuven, Belgium
(Received 8 September 1995)

In-plane electronic transport in ultrathin metallic magnetic structures composed of two ferromagnetic films separated by a nonmagnetic metallic spacer is analyzed theoretically, with particular attention paid to the role of quantum size phenomena and interface roughness in the giant magnetoresistance (GMR) effect. Within the one-band model we predict oscillations in the resistivity and GMR as a function of the spacer thickness. In general, two different oscillation periods are found. It is also shown that the spin-dependent scattering due to interface roughness can enhance or reduce the GMR effect generated by the spin-dependent scattering on impurities or other defects inside the films. Long-range in-plane structural correlations of the interface roughness reduce its role in the GMR effect.

I. INTRODUCTION

The current-in-plane (CIP) giant magnetoresistance (GMR) effect in magnetic multilayers consists in a large change of the in-plane electrical resistance as the magnetizations of neighboring magnetic films rotate from the antiparallel to parallel alignment.[1,2] The effect has been observed in many structures which include transition-metal magnetic films.[3] Antiparallel alignment can easily be obtained if there is an antiferromagnetic-type exchange coupling between the magnetic films. However, the existence of an interlayer coupling is not a necessary condition for the GMR to occur, and antiparallel alignment can also be obtained by other methods.[4]

In most cases investigated experimentally there was a drop in the resistance as the film magnetizations rotated from antiparallel to parallel alignment (normal effect), but an increase of the resistance (inverse effect) was also observed.[5] The effect is usually described quantitatively by the ratio $\Delta\rho/\rho_{\mathrm{P}}$, where $\Delta\rho=\rho_{\mathrm{AP}}-\rho_{\mathrm{P}}$, whereas ρ_{AP} and ρ_{P} are the resistivities, respectively, in the antiparallel and parallel configurations. The normal (inverse) effect corresponds then to a positive (negative) value of $\Delta\rho/\rho_{\mathrm{P}}$. From the point of view of the conventional definition of magnetoresistance, the normal and inverse GMR effects correspond, respectively, to a negative and positive magnetoresistance.

The largest relative resistance change due to the magnetization rotation was found in $[\mathrm{Fe}(4.5)/\mathrm{Cr}(12)]_{50}$ superlattices, where $\Delta\rho/\rho_{\mathrm{P}}=2.2$ at 1.5 K.[6] We use here the notation $[A(x)/B(y)]_n$, where x and y are the thicknesses, respectively, of the material A and B (measured in angstroms) and n is the number of bilayers.

The most important characteristics of the GMR effect are (i) the temperature dependence, (ii) the dependence on the number of films in a multilayer, and (iii) the dependence on the thickness of magnetic and nonmagnetic sublayers. The GMR effect decreases with increasing temperature, but the rate of the decrease depends on the composition and type of the structure. In the case of Fe/Cr multilayers, the GMR effect decreases rather fast with increasing temperature. In $[\mathrm{Fe}(4.5)/\mathrm{Cr}(12)]_{50}$ superlattices[6] $\Delta\rho/\rho_{\mathrm{P}}=0.42$ at 300 K, while $\Delta\rho/\rho_{\mathrm{P}}=2.2$ at 1.5 K. In Co/Cu multilayers, however, $\Delta\rho/\rho_{\mathrm{P}}$ decreases less fast with increasing temperature, and so in the $[\mathrm{Co}(10)/\mathrm{Cu}(10)]_{100}$ multilayers $\Delta\rho/\rho_{\mathrm{P}}=0.8$ at 300 K,[7] which, to our knowledge, is the highest value reported up to now at room temperature. The GMR effect also decreases with increasing spacer thickness d_0 and disappears when d_0 is significantly larger than the bulk electron mean free path in the spacer material. The dependence on the thickness d_m of the magnetic films is more complex. The GMR disappears in the two opposite limits, i.e., for $d_m\rightarrow 0$, and also for sufficiently thick magnetic films. At a certain value of d_m, smaller than the corresponding electron mean free paths, the GMR reaches a maximum. When the sublayer thicknesses are much smaller than the electron mean free paths, then the GMR effect considerably increases with increasing number of films in a multilayer.

The GMR effect can be explained qualitatively and described quantitatively by taking into account a spin asymmetry of the parameters describing transport properties of the two spin channels for electronic conduction.[4,8,9] At low temperatures the channels can be considered as independent. At higher temperatures, however, one has to take into account interchannel transitions, particularly those which almost conserve the electron momentum.[10]

Two factors contribute to the spin asymmetry of the two channels: the spin dependence of the scattering probabilities and the spin dependence of the electronic structure of a defect-free system. However, those two factors are not independent because the spin-dependent electronic structure contributes also to the spin dependence of the scattering probabilities. This is due to the fact that the spin asymmetry in scattering rates results not only from the spin dependence of the scattering potentials, but also from the spin asymmetry of the density of electron states at the Fermi level. In general, one can distinguish between two types of the scattering potential: the so-called bulk scattering potential, which originates from impurities and defects located inside the ferromagnetic and nonmagnetic films, and the interface scattering potential due to a geometrical interface roughness or due to intermixing effects. The scattering potential itself, particularly that of a rough interface, also depends on the electronic band structure. In the diffuse limit the contributions from the spin-dependent scattering rates and spin-dependent band

structure are not separable. In systems which are free of scattering defects (limit of ballistic transport), the situation can change and the GMR effect can be entirely due to the spin dependence of the electronic band structure.[11]

Two approaches have been developed for the theoretical description of the CIP transport phenomena in magnetic multilayers: the quasiclassical one based on the Boltzmann kinetic equation[4,8,12–14] and the quantum-mechanical Kubo formalism in real[15–18] and reciprocal[9] spaces. All those approaches are based on the one-band free-electron-like approximation for conduction electrons. Another theoretical approach developed recently is based on the one-band tight-binding model.[19–21]

Since the GMR effect is not of a quantum origin, the quasiclassical approach gives rather satisfactory results, except in the limit of very clean sublayers, when the bulk electron mean free paths are much longer than the sublayer thicknesses. In that limit the quasiclassical approach breaks down and one has to apply a quantum-mechanical formalism, which explicitly takes into account the wave nature of electrons. This, in turn, leads to quantum size effects in the resistivity and magnetoresistance. Those effects give rise to oscillations in the dependence of the resistivity of a single metallic film on the film thickness.[22,23] They also lead to similar oscillations in the GMR effect in magnetic sandwich structures.[15,18]

Without counting the role of interfaces in the breakdown of the quasiclassical approach in the limit of infinite bulk mean free paths, the role of the interfacial roughness itself in the GMR effect is still not clear. Much experimental work has been done[24–27] to clarify the role of interface roughness, but it is still not clear which scattering processes, bulk or interface, contribute dominantly to the observed GMR effect. Apparently, both contributions are important and their relative role depends on such factors like the quality of the interfaces, distribution of bulk scattering centers, composition of the multilayers, and possibly other factors.

In this paper we consider a sandwich structure with two ferromagnetic films separated by a nonmagnetic spacer. Electronic transport properties are described within the two-current Mott model,[28] with particular attention paid to the role of interface roughness and quantum size effects in the GMR effect.[29] We consider the case when the Fermi level is adjusted so that the number N^{el} of conduction electrons per unit area of the structure varies with the sublayer thicknesses as $N^{\mathrm{el}}=\Sigma_\alpha n_\alpha d_\alpha$, where n_α are the bulk electron concentrations and d_α are the sublayer thicknesses (the index α distinguishes here between different sublayers, $\alpha=0,1,2$, with $\alpha=0$ corresponding to the spacer and $\alpha=1,2$ to the two magnetic films). We show that the size effects lead to oscillations in the dependence of the resistivity and GMR effect on the spacer thickness with two different oscillation periods, in general. One of them is related to the Fermi wave vector and was already found before.[15,18] The other one occurs in the presence of interface roughness and is related to the depth of the quantum well in the spacer. We also show that the spin-dependent scattering by a small interface roughness can either enhance or reduce the GMR effect generated by the spin-dependent bulk scattering.

In Sec. II we describe briefly the model used for the theoretical description of the transport properties of magnetic multilayers. In Sec. III the appropriate formula for the electronic conductivity is derived. Numerical results are presented and discussed in Sec. IV, whereas some general conclusions are given in Sec. V.

II. DESCRIPTION OF THE MODEL

The structure under consideration consists of two ferromagnetic layers of thicknesses d_1 and d_2, which are separated by a nonmagnetic film of thickness d_0. Let the axis z be normal to the structure and $\vec{R}$ be the two-dimensional in-plane position vector ($\vec{r}\equiv[\vec{R},z]$). The two interfaces (indexed in the following with β, $\beta=1,2$) are assumed to be located at $z=z_\beta(\vec{R})$, with

$$z_\beta(\vec{R})=z_\beta+f_\beta(\vec{R}). \tag{1}$$

Here $z_1=d_1$, $z_2=d_1+d_0$, and the function $f_\beta(\vec{R})$ describes deviation of the βth interface from the perfectly flat plane $z=z_\beta$, with

$$\langle f_\beta(\vec{R})\rangle=\frac{1}{S}\int f_\beta(\vec{R})d\vec{R}=0, \tag{2}$$

by definition, where S is the sample area and $\langle A\rangle$ denotes the average value of the quantity A.

In real structures the functions $f_\beta(\vec{R})$ taken at two different points of the same or different interfaces are usually correlated. In this paper, however, we will consider the case of no correlation between the roughness of different interfaces (no cross correlations). Moreover, we assume that both interfaces are described by the same autocorrelation function $G(R/\xi)$,

$$\langle f_\beta(\vec{R}')f_{\beta'}(\vec{R}'+\vec{R})\rangle=\frac{1}{S}\int f_\beta(\vec{R}')f_{\beta'}(\vec{R}'+\vec{R})d\vec{R}'$$
$$=\delta_{\beta\beta'}\eta_\beta^2 G(R/\xi_\beta), \tag{3}$$

where η_β is the amplitude of the interface roughness,

$$\eta_\beta=\langle f_\beta^2(\vec{R})\rangle^{1/2}=\left[\frac{1}{S}\int f_\beta^2(\vec{R})d\vec{R}\right]^{1/2}, \tag{4}$$

and ξ_β is the lateral correlation length. We assume the same form of the autocorrelation function $G(R/\xi)$ for both interfaces, but the roughness amplitude η_β and the correlation length ξ_β can be different for different interfaces, $\eta_1\neq\eta_2$ and $\xi_1\neq\xi_2$, in general. In the following we will assume the exponential model for the autocorrelation function,

$$G(R/\xi)=\exp(-R/\xi). \tag{5}$$

For simplicity, we assume perfect outer surfaces which are located, respectively, at $z=0$ and $z=d_1+d_0+d_2\equiv L$, with L being the total thickness of the structure.

The electronic properties of the structure under consideration will be described within the one-band model, with the conduction band of the ferromagnetic metal being spin split due to an effective exchange field. No spin split is assumed for the nonmagnetic spacer. We assume further that impurities with a spin-dependent scattering potential are distributed uniformly inside the magnetic films. The scattering potential of impurities located inside the nonmagnetic spacer is as-

sumed to be independent of the electron spin orientation. For simplicity, we will consider only configurations with strictly parallel and antiparallel magnetizations and will neglect spin-flip scattering processes. The two spin channels for electronic transport can then be considered separately.

The electron states of a given spin orientation σ are described by the total Hamiltonian H_σ of the form

$$H_\sigma = H_{0\sigma}(\vec{r}) + V_\sigma(\vec{r}), \tag{6}$$

where $H_{0\sigma}(\vec{r})$ is the Hamiltonian of the defect-free system,

$$H_{0\sigma}(\vec{r}) = -\frac{\hbar^2}{2m}\nabla^2 + U_\sigma(z), \tag{7}$$

with a steplike effective electron potential

$$U_\sigma(z) = \begin{cases} U_{1\sigma}, & 0 \leqslant z \leqslant d_1, \\ U_{0\sigma} = U_0 = 0, & d_1 < z \leqslant d_1 + d_0, \\ U_{2\sigma}, & d_1 + d_0 < z \leqslant L, \end{cases} \tag{8}$$

where $U_{1\sigma}$ and $U_{2\sigma}$ are constants, which depend on the electron spin, and $U_{1\sigma}, U_{2\sigma} \geqslant U_0$ for simplicity. Infinite potential walls are assumed at the outer surfaces, i.e., for $z<0$ and $z>L$. The effective electron potential for both magnetization orientations and for both spin directions is shown schematically in Fig. 1. According to our notation, the electron spin projection onto the global quantization axis is denoted as $\sigma=\uparrow$ for $s_z=1/2$ and $\sigma=\downarrow$ for $s_z=-1/2$. The spin projection on the local quantization axis (direction opposite to the local magnetization) is denoted as $+$ for the spin-majority electrons and $-$ for the spin-minority electrons. In Eq. (6), $V_\sigma(\vec{r})$ is a scattering potential due to impurities and interface roughness. Assuming the contact form of the impurity potential, we write $V_\sigma(\vec{r})$ as

$$V_\sigma(\vec{r}) = \sum_{i\alpha} v_{\alpha\sigma}\delta(\vec{r} - \vec{r}_{i\alpha}) - \sum_\beta f_\beta(\vec{R}) V^{\text{eff}}_{\beta\sigma}\delta[z - z^c_\beta(\vec{R})], \tag{9}$$

with $v_{\alpha\sigma}$ denoting the spin-dependent scattering potential of an impurity located inside the αth layer ($\alpha=0,1,2$) and $z^c_\beta(\vec{R})$ being the location center of the interface scattering potential, $z^c_\beta(\vec{R}) = z_\beta + (1/2) f_\beta(\vec{R})$. For each α the index i in the first term on the right-hand side runs over all impurities distributed inside the αth film. According to our assumption, $v_{0\sigma}$ is independent of the electron spin, $v_{0\sigma}=v_0$. The effective interface scattering potential $V^{\text{eff}}_{\beta\sigma}$ in Eq. (9) consists of two terms $V^{\text{eff}}_{\beta\sigma} = V_{\beta\sigma} + \tilde{V}_{\beta\sigma}$, where $\tilde{V}_{\beta\sigma}$ describes effectively those s-d scattering processes which are induced by the interface roughness and $V_{\beta\sigma}$ is the potential step at the βth interface, $V_{\beta\sigma} = U_{\beta\sigma} - U_0$. If $\tilde{V}_{\beta\sigma}=0$, then only s-s-type scattering processes induced by the interface roughness are taken into account. The interference effects due to electron scattering by those two different terms in $V^{\text{eff}}_{\beta\sigma}$ will be neglected.

The Hamiltonian $H_{0\sigma}$ describes electrons in a quantum well with perfect interfaces and surfaces and with the electron potential shown schematically in Fig. 1. For a given configuration the eigenstates $\langle \vec{r} | \mu \vec{q} \sigma \rangle$ of $H_{0\sigma}$ are of the form

$$\langle \vec{r} | \mu \vec{q} \sigma \rangle = \frac{1}{\sqrt{S}} \psi_{\mu\sigma}(z) e^{i\vec{q}\cdot\vec{R}}, \tag{10}$$

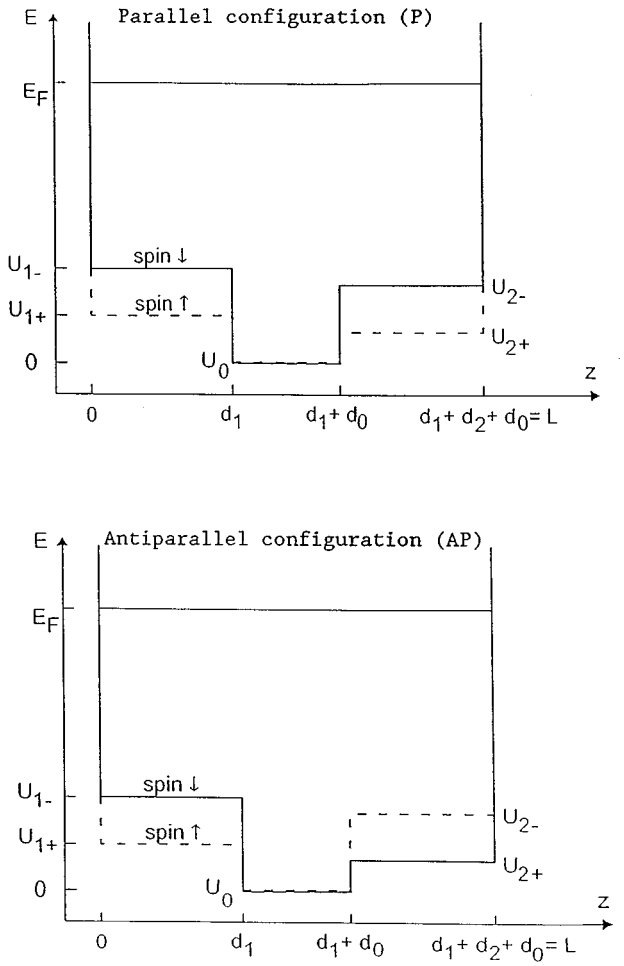

FIG. 1. Potential profiles for both $\sigma=\uparrow$ and $\sigma=\downarrow$ spin directions in the parallel (P) and antiparallel (AP) configurations.

with the corresponding eigenvalues,

$$\epsilon_{\mu\sigma}(\vec{q}) = \epsilon_{\mu\sigma} + \frac{\hbar^2 q^2}{2m}. \tag{11}$$

The index μ distinguishes here different electron minibands, $\vec{q}$ is the in-plane wave vector, $\epsilon_{\mu\sigma}$ are the discrete energy levels arising from the quantization of perpendicular motion, and $\psi_{\mu\sigma}(z)$ are the corresponding normalized wave functions. Equations for $\psi_{\mu\sigma}(z)$ and $\epsilon_{\mu\sigma}$ are given in Appendix A.

III. CONDUCTIVITY

The electronic spectrum of the structure under consideration consists of a set of two-dimensional minibands (or subbands). The scattering processes due to impurities and interface roughness lead to intra- as well as interminiband transitions, which gives rise to the electrical resistance. To find the resistance we extend the method developed by Calecki.[23]

Consider a particular magnetization configuration. The stationary nonequilibrium distribution functions $f_{\mu\sigma}(\vec{q})$ for electrons with spin σ and in the state $\vec{q}$ of the μth miniband obey the following set of coupled Boltzmann equations:[23]

$$-\frac{e}{\hbar}\vec{E}\cdot\nabla_{\vec{q}}f_{\mu\sigma}(\vec{q})=\sum_{\mu'}\sum_{\vec{q}'}\sum_{\sigma'}\{W^{\mu\sigma}_{\mu'\sigma'}(\vec{q}',\vec{q})f_{\mu'\sigma'}(\vec{q}')\times[1-f_{\mu\sigma}(\vec{q})]-W^{\mu'\sigma'}_{\mu\sigma}(\vec{q},\vec{q}')f_{\mu\sigma}(\vec{q})\times[1-f_{\mu'\sigma'}(\vec{q}')]\},\quad(12)$$

where $\vec{E}$ is the driving electric field applied in the film plane, $-e$ is the electron charge, and $W^{\mu'\sigma'}_{\mu\sigma}(\vec{q},\vec{q}')$ is the probability per unit time for an electron to pass from the state $|\mu\vec{q}\sigma\rangle$ to the state $|\mu'\vec{q}'\sigma'\rangle$. In the following we will consider only spin-conserving scattering processes, i.e.,

$$W^{\mu'\sigma'}_{\mu\sigma}(\vec{q},\vec{q}')=W^{\mu'\sigma'}_{\mu\sigma}(\vec{q},\vec{q}')\delta_{\sigma\sigma'}\equiv W^{\sigma}_{\mu\mu'}(\vec{q},\vec{q}')\delta_{\sigma\sigma'}.\quad(13)$$

This approximation is reasonable for low temperatures. Moreover, we restrict considerations to the elastic scattering processes only. With this assumption one may write $W^{\sigma}_{\mu\mu'}(\vec{q},\vec{q}')$ as

$$W^{\sigma}_{\mu\mu'}(\vec{q},\vec{q}')=P^{\sigma}_{\mu\mu'}(\vec{q},\vec{q}')\delta[\epsilon_{\mu\sigma}(\vec{q})-\epsilon_{\mu'\sigma}(\vec{q}')],\quad(14)$$

where, in the Born approximation, $P^{\sigma}_{\mu\mu'}(\vec{q},\vec{q}')$ is given by

$$P^{\sigma}_{\mu\mu'}(\vec{q},\vec{q}')=P^{\sigma}_{\mu\mu'}(|\vec{q}-\vec{q}'|)=\frac{2\pi}{\hbar}|\langle\mu\vec{q}\sigma|V_{\sigma}|\mu'\vec{q}'\sigma\rangle|^2.\quad(15)$$

It has been assumed above that the electron scattering processes are isotropic in the film plane; i.e., $P^{\sigma}_{\mu\mu'}(\vec{q},\vec{q}')$ depends only on $|\vec{q}-\vec{q}'|$.

To solve Eq. (12) one writes the distribution function $f_{\mu\sigma}(\vec{q})$ as a sum of the equilibrium Fermi-Dirac distribution $f^0[\epsilon_{\mu}(\vec{q})]$ and the deviation from the equilibrium, $\Phi_{\mu\sigma}(\vec{q})$,

$$f_{\mu\sigma}(\vec{q})=f^0_{\mu\sigma}[\epsilon_{\mu\sigma}(\vec{q})]+\Phi_{\mu\sigma}(\vec{q}).\quad(16)$$

In a general case, the functions $\Phi_{\mu\sigma}(\vec{q})$ can be written in the form

$$\Phi_{\mu\sigma}(\vec{q})=-\frac{e\hbar}{m}\vec{q}\cdot\vec{E}\frac{\partial f^0[\epsilon_{\mu\sigma}(\vec{q})]}{\partial[\epsilon_{\mu\sigma}(\vec{q})]}g_{\mu\sigma}[\epsilon_{\mu\sigma}(\vec{q})].\quad(17)$$

On substituting (16) and (17) into Eq. (12), one obtains a set of equations for the functions $g_{\mu\sigma}[\epsilon_{\mu\sigma}(\vec{q})]$. For a particular energy ϵ, one can write the solution of this set of equations in the matrix form as

$$\mathbf{g}_{\sigma}(\epsilon)=-\mathbf{C}^{-1}_{\sigma}(\epsilon)\mathbf{F}_{\sigma}(\epsilon),\quad(18)$$

where $\mathbf{g}_{\sigma}(\epsilon)$ is a column matrix with the matrix elements $[\mathbf{g}_{\sigma}(\epsilon)]_{\mu}=g_{\mu\sigma}(\epsilon)$ and $\mathbf{F}_{\sigma}(\epsilon)$ is also a column matrix with the μth element defined as

$$[\mathbf{F}_{\sigma}(\epsilon)]_{\mu}=\frac{m}{\hbar^2}N_{\mu\sigma}(\epsilon)(\epsilon-\epsilon_{\mu\sigma}).\quad(19)$$

Here $N_{\mu\sigma}(\epsilon)$ is the density of electron states for spin σ in the subband μ,

$$N_{\mu\sigma}(\epsilon)=\frac{Sm}{\pi\hbar^2}\Theta(\epsilon-\epsilon_{\mu\sigma}),\quad(20)$$

with $\Theta(x)=1$ for $x\geqslant 0$ and $\Theta(x)=0$ for $x<0$. Finally, the components of the matrix $\mathbf{C}_{\sigma}(\epsilon)$ in Eq. (18) are of the form

$$[\mathbf{C}_{\sigma}(\epsilon)]_{\mu\mu'}=\delta_{\mu\mu'}\sum_{\nu}\sum_{\vec{q}}\sum_{\vec{q}'}q^2P_{\mu\nu}(|\vec{q}-\vec{q}'|)\delta[\epsilon-\epsilon_{\mu\sigma}(\vec{q})]\delta[\epsilon-\epsilon_{\nu\sigma}(\vec{q}')]-\sum_{\vec{q}}\sum_{\vec{q}'}(\vec{q}\cdot\vec{q}')P_{\mu\mu'}(|\vec{q}-\vec{q}'|)\delta[\epsilon-\epsilon_{\mu\sigma}(\vec{q})]\delta[\epsilon-\epsilon_{\mu'\sigma}(\vec{q}')].\quad(21)$$

The order of the matrices $\mathbf{C}_{\sigma}(\epsilon)$, $\mathbf{g}_{\sigma}(\epsilon)$, and $\mathbf{F}_{\sigma}(\epsilon)$ is determined by the number of discrete levels with $\epsilon_{\mu\sigma}<\epsilon$.

The averaged current density for spin σ is given by the formula

$$\vec{j}_{\sigma}=-\frac{e\hbar}{SL}\sum_{\mu}\sum_{\vec{q}}\frac{\vec{q}}{m}\Phi_{\mu\sigma}(\vec{q}).\quad(22)$$

Taking into account (17) and calculating the appropriate matrix elements for the transition probabilities, one arrives at the following formula for the zero-temperature global in-plane conductivity $g_{\parallel}$:

$$g_{\parallel}=\frac{e^2Sm^2}{2\pi^2\hbar^6L}\sum_{\sigma}\sum_{\mu=1}^{N_{\sigma}}\sum_{\mu'=1}^{N_{\sigma}}(E_F-\epsilon_{\mu\sigma})(E_F-\epsilon_{\mu'\sigma})[\mathbf{C}^{-1}_{\sigma}(E_F)]_{\mu\mu'},\quad(23)$$

where E_F is the Fermi energy and N_{σ} is the number of occupied minibands for spin σ.

The impurity contribution to the matrix $\mathbf{C}_{\sigma}(E_F)$, averaged over the impurity distribution, can be calculated rather easily. Some problems arise when considering the contribution due to scattering by the rough interfaces. When calculating transition probabilities between different states, one has to evaluate the average

$$M^{\nu\mu}_{\beta\sigma}(\vec{q},\vec{q}')=\int d\vec{R}\int d\vec{R}'\;e^{i(\vec{q}-\vec{q}')\cdot\vec{R}'}\langle f_{\beta}(\vec{R})f_{\beta}(\vec{R}+\vec{R}')\psi_{\nu\sigma}[z=z^c_{\beta}(\vec{R})]\psi_{\mu\sigma}[z=z^c_{\beta}(\vec{R})]\psi_{\nu\sigma}[z=z^c_{\beta}(\vec{R}+\vec{R}')]\times\psi_{\mu\sigma}[z=z^c_{\beta}(\vec{R}+\vec{R}')]\rangle.\quad(24)$$

To find $M_{\beta\sigma}^{\nu\mu}(\vec{q},\vec{q}')$ we expand the wave functions in a power series of $f_\beta(\vec{R})$, as

$$\psi_{\nu\sigma}[z=z_\beta^c(\vec{R})]\approx\psi_{\nu\sigma}(z_\beta)+\tfrac{1}{2}f_\beta(\vec{R})\psi'_{\nu\sigma}(z_\beta)+\cdots, \tag{25}$$

where $\psi'_{\nu\sigma}(z_\beta)$ is the first derivative of $\psi_{\nu\sigma}(z_\beta)$. In the following we will take into account only the first two terms. To find the average in Eq. (24), we will make use of the approximations

$$\langle f_\beta^3(\vec{R})f_\beta(\vec{R}+\vec{R}')\rangle\approx\eta_\beta^2\langle f_\beta(\vec{R})f_\beta(\vec{R}+\vec{R}')\rangle \tag{26}$$

and

$$\langle f_\beta^2(\vec{R})f_\beta^2(\vec{R}+\vec{R}')\rangle\approx\eta_\beta^4. \tag{27}$$

Taking into account the above approximations, one finds the matrix elements $[\mathbf{C}_\sigma(E_F)]_{\mu\mu'}$ in the form

$$\begin{aligned}[\mathbf{C}_\sigma(E_F)]_{\mu\mu'}=\frac{Sm^2}{4\pi^2\hbar^5}\Bigg[\delta_{\mu\mu'}\sum_{\nu=1}^{N_\sigma}Q_{\mu\sigma}^2\Bigg(&2\pi n_1^{\rm imp}v_{1\sigma}^2K_{1\sigma}^{\mu\nu}+2\pi n_0^{\rm imp}v_{0\sigma}^2K_{0\sigma}^{\mu\nu}+2\pi n_2^{\rm imp}v_{2\sigma}^2K_{2\sigma}^{\mu\nu}\\&+(V_{1\sigma}^2+\tilde{V}_{1\sigma}^2)(\eta_1\xi_1)^2L_{1\sigma}^{\mu\nu}\int_0^{2\pi}d\theta\,F(\xi_1Q_{\mu\nu\sigma})+(V_{2\sigma}^2+\tilde{V}_{2\sigma}^2)(\eta_2\xi_2)^2L_{2\sigma}^{\mu\nu}\int_0^{2\pi}d\theta\,F(\xi_2Q_{\mu\nu\sigma})\Bigg)\\&-Q_{\mu\sigma}Q_{\mu'\sigma}\int_0^{2\pi}d\theta\,\cos\theta[(V_{1\sigma}^2+\tilde{V}_{1\sigma}^2)(\eta_1\xi_1)^2L_{1\sigma}^{\mu\mu'}F(\xi_1Q_{\mu\mu'\sigma})\\&+(V_{2\sigma}^2+\tilde{V}_{2\sigma}^2)(\eta_2\xi_2)^2L_{2\sigma}^{\mu\mu'}F(\xi_2Q_{\mu\mu'\sigma})]\Bigg],\end{aligned} \tag{28}$$

where $Q_{\mu\mu'\sigma}$ is defined as

$$Q_{\mu\mu'\sigma}=(Q_{\mu\sigma}^2+Q_{\mu'\sigma}^2-2Q_{\mu\sigma}Q_{\mu'\sigma}\cos\theta)^{1/2}, \tag{29}$$

with $Q_{\mu\sigma}$ being the in-plane Fermi wave vector in the corresponding μth miniband for spin σ. The first three terms in Eq. (28) originate from scattering on impurities with the scattering potential $v_{\alpha\sigma}$ and concentration $n_\alpha^{\rm imp}$ (for $\alpha=0,1,2$). We assumed here a uniform distribution of the impurities inside each sublayer. The factors $K_{\alpha\sigma}^{\mu\nu}$ are defined as

$$K_{\alpha\sigma}^{\mu\nu}=\int_{(d_\alpha)}dz\;\psi_{\mu\sigma}^2(z)\psi_{\nu\sigma}^2(z), \tag{30}$$

where the integration is over z ranging the αth sublayer. Explicit forms of $K_{\alpha\sigma}^{\mu\nu}$ are given in Appendix B. The other terms in Eq. (28) result from the scattering on both interfaces with $L_{1\sigma}^{\mu\mu'}$ and $L_{2\sigma}^{\mu\mu'}$ defined as

$$L_{1\sigma}^{\mu\mu'}=[\psi_{\mu\sigma}(d_1)\psi_{\mu'\sigma}(d_1)+\tfrac{1}{4}\eta_1^2\psi'_{\mu\sigma}(d_1)\psi'_{\mu'\sigma}(d_1)]^2 \tag{31}$$

and

$$\begin{aligned}L_{2\sigma}^{\mu\mu'}=[&\psi_{\mu\sigma}(d_1+d_0)\psi_{\mu'\sigma}(d_1+d_0)\\&+\tfrac{1}{4}\eta_2^2\psi'_{\mu\sigma}(d_1+d_0)\psi'_{\mu'\sigma}(d_1+d_0)]^2.\end{aligned} \tag{32}$$

Finally, $F(\xi Q)$ in Eq. (28) is the Fourier transform of the autocorrelation function (5),

$$F(\xi q)=2\pi(1+\xi^2q^2)^{-3/2}. \tag{33}$$

It is convenient to rewrite the expression for the conductivity in the form

$$g_\parallel=\frac{e^2\hbar^3}{2m^2L}\sum_\sigma\sum_{\mu=1}^{N_\sigma}\sum_{\mu'=1}^{N_\sigma}Q_{\mu\sigma}^2Q_{\mu'\sigma}^2[\tilde{\mathbf{C}}_\sigma^{-1}(E_F)]_{\mu\mu'}, \tag{34}$$

where $\tilde{\mathbf{C}}_\sigma$ is related to the matrix $\mathbf{C}_\sigma$ by the equation

$$\tilde{\mathbf{C}}_\sigma=\frac{4\pi^2\hbar^5}{Sm^2}\,\mathbf{C}_\sigma. \tag{35}$$

Equations (28), (34), and (35) are our final results for the electrical conductivity.

IV. NUMERICAL RESULTS

In the preceding section we derived the general formulas for the electrical conductivity of a magnetic sandwich structure with both interface and bulk scattering included. To find the ratio $\Delta\rho/\rho_{\rm P}$, one has to calculate first the resistivity for both parallel and antiparallel configurations. When considering the problem numerically, one has to take into account the variation of the Fermi level with the sublayer thicknesses and also a change of the level as the film magnetizations rotate from antiparallel to parallel alignment. In each case the Fermi level will be adjusted to keep the areal electron density $N^{\rm el}$ according to the formula

$$N^{\rm el}=\sum_{\alpha=0,1,2}n_\alpha d_\alpha=\sum_{\alpha=0,1,2}(n_{\alpha+}+n_{\alpha-})d_\alpha, \tag{36}$$

where $n_{\alpha\sigma}$ is the bulk electron concentration for spin σ in the αth material. The electron density in the spacer material is

independent of the spin orientation, $n_{0\pm}=n_0/2$. The bulk electron concentrations are determined by $\mu_{\alpha\pm}=\mu-U_{\alpha\pm}$, where μ is the common chemical potential.

Consider now some numerical results, and let us start with the simplest case, when the electron potential is uniform across the structure.

A. Constant electron potential

We consider here the situation when $U_{1\pm}=U_0=U_{2\pm}=0$. In that case the interface roughness can influence the resistance and also the magnetoresistance only in the case of nonvanishing potentials $\tilde{V}_{1\pm}$ and $\tilde{V}_{2\pm}$. Suppose first that the interfaces are perfectly flat, i.e., $\eta_1=\eta_2=0$. The only contribution to the resistance comes then from the electron scattering on impurities distributed inside the films. If the scattering potential of the impurities in the magnetic films is spin dependent, then there is also a nonvanishing resistance change due to the magnetization rotation. As basic parameters describing the bulk scattering, we will use in the following the electron mean free paths, which are determined by the impurity potentials and impurity concentrations.

In Fig. 2 we show the resistivity in the parallel (ρ_{P}) and antiparallel (ρ_{AP}) configurations (a), the resistivity change $\Delta\rho=\rho_{\mathrm{AP}}-\rho_{\mathrm{P}}$ (b), and the relative resistivity change $\Delta\rho/\rho_{\mathrm{P}}$ (c). Both ρ_{P} and ρ_{AP} show well-defined oscillations with increasing spacer thickness d_0, which originate from quantum size effects due to external boundaries. The period Λ of the saw-shaped oscillations is determined by the Fermi wavelength λ_F as $\Lambda=\lambda_F/2$. The oscillations in ρ_{P} and ρ_{AP} result in a similar fine structure in the dependence of the resistivity change $\Delta\rho$ on the spacer thickness d_0, as is clearly evident in part (b). However, the oscillations in the resistivity ρ_{P} and in the resistivity change $\Delta\rho$ cancel each other, and so there is no fine structure in the factor $\Delta\rho/\rho_{\mathrm{P}}$. This factor decreases exponentiallylike with increasing spacer thickness.[15] A similar behavior can also be observed in the dependence of the resistivity, resistivity change, and GMR on the thickness of one of the magnetic films, say, on d_2, as shown in Fig. 3 for constant d_1 and d_0. The resistivities ρ_{P} and ρ_{AP} as well as the resistivity change $\Delta\rho$ oscillate with increasing d_2. However, the oscillations disappear in the factor Δ/ρ_{P}. Contrary to the d_0 dependence [Fig. 2(c)], $\Delta\rho/\rho_{\mathrm{P}}$ increases now smoothly with increasing d_2 and then, after reaching a maximum at some value of d_2, decreases with a further increase of the thickness of the magnetic film.[15,18]

Consider now the role of interface roughness. Since the electron potential is uniform across the structure, the roughness can play a significant role only for nonvanishing scattering potentials $\tilde{V}_{1\pm}$ and $\tilde{V}_{2\pm}$. If $\tilde{V}_{1\pm}$ and $\tilde{V}_{2\pm}$ are spin dependent, then they also contribute to the magnetoresistance. Figure 4 shows the dependence of $\Delta\rho/\rho_{\mathrm{P}}$ on the spacer thickness d_0 in the case when the magnetoresistance is generated entirely by the spin-dependent scattering potentials $\tilde{V}_{1\pm}$ and $\tilde{V}_{2\pm}$, i.e., when there is no spin asymmetry in the bulk scattering processes. The fine oscillations in $\Delta\rho/\rho_{\mathrm{P}}$ are due to quantum size effects and are quite significant, contrary to the case when the magnetoresistance is generated only by the bulk spin-dependent scattering [see Fig. 2(c)].

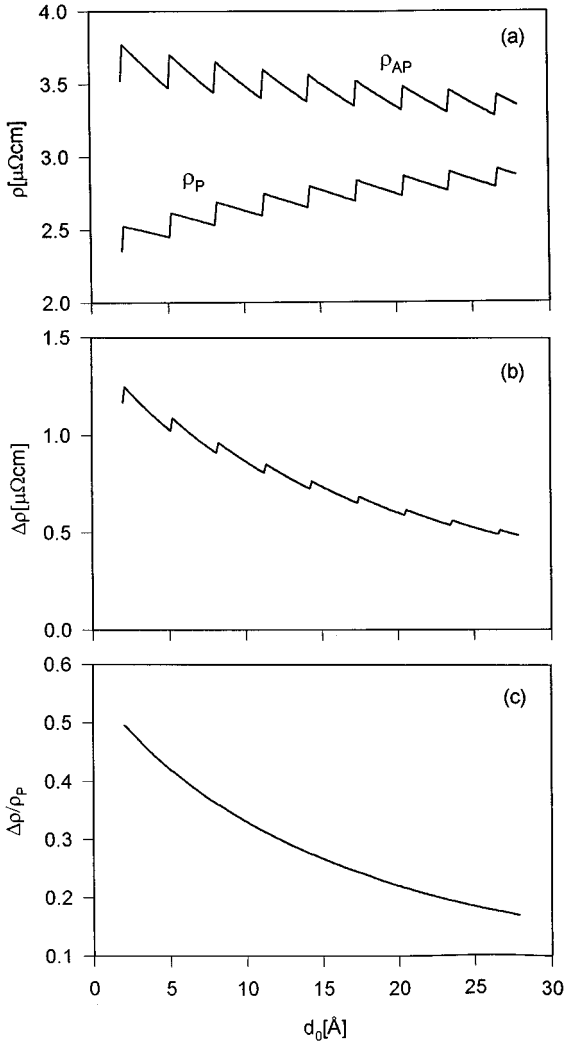

FIG. 2. (a) Electrical resistivities ρ_{P} and ρ_{AP}, (b) the resistance change $\Delta\rho$, and (c) the GMR effect as a function of the spacer thickness d_0 calculated for $d_1=d_2=20$ Å, $U_{1\pm}=U_{2\pm}=U_0=0$, $\mu=4$ eV, $\lambda_{1-}=\lambda_{2-}=200$ Å, $\lambda_{1+}=\lambda_{2+}=800$ Å, $\lambda_0=400$ Å, and $\eta_1=\eta_2=0$.

B. Spin-independent quantum well in the spacer

Assume now that the electron potential in the magnetic films is independent of the electron spin and $U_{1\pm},U_{2\pm}>U_0$ ($U_0=0$). This corresponds to a situation when there is a quantum well in the spacer, which is the same for both electron spin orientations.

Consider first the case of no interface roughness. The only contribution to the GMR effect is then due to the spin-dependent bulk electron scattering. The dependence of the resistivities ρ_{P} and ρ_{AP} on the spacer thickness d_0 and on the thickness of the ferromagnetic films is similar to that in the case of no quantum well in the spacer, i.e., similar to the variations shown, respectively, in Figs. 2(a) and 3(a). Also, the magnetoresistance behaves in a similar way: i.e., it decreases smoothly with increasing spacer thickness d_0, as shown in Fig. 5. Thus the existence of a quantum well does not lead to new features in the dependence of the magnetoresistance on the thickness of magnetic and/or nonmagnetic films.

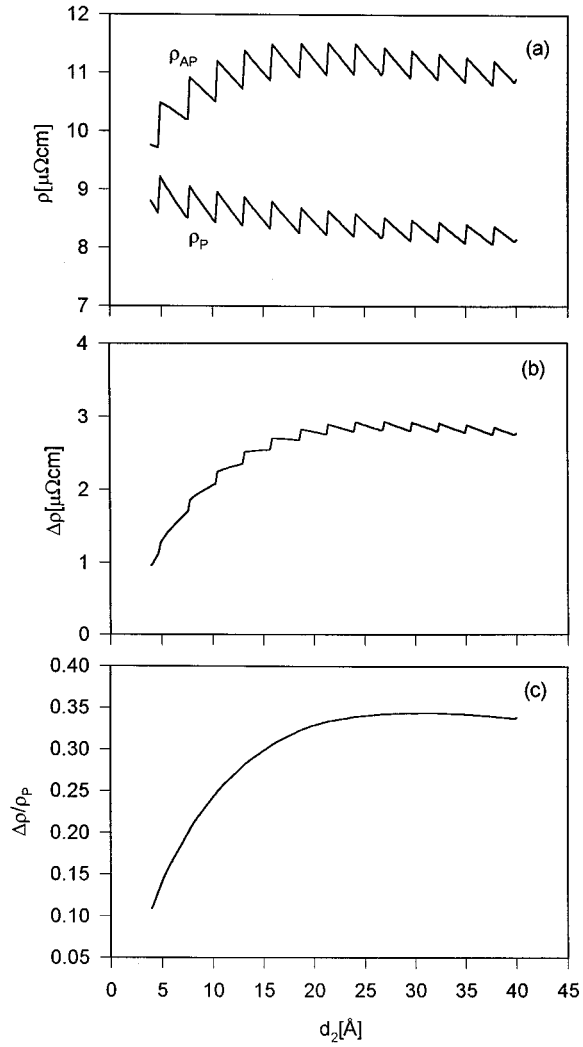

FIG. 3. (a) Electrical resistivities ρ_P and ρ_{AP}, (b) the resistance change, and (c) the GMR effect as a function of the thickness d_2 of the ferromagnetic film, calculated for $d_1=20$ Å, $d_0=10$ Å, $U_{1\pm}=U_{2\pm}=U_0=0$, $\mu=5$ eV, $\lambda_{1-}=\lambda_{2-}=200$ Å, $\lambda_{1+}=\lambda_{2+}=50$ Å, $\lambda_0=100$ Å, and $\eta_1=\eta_2=0$.

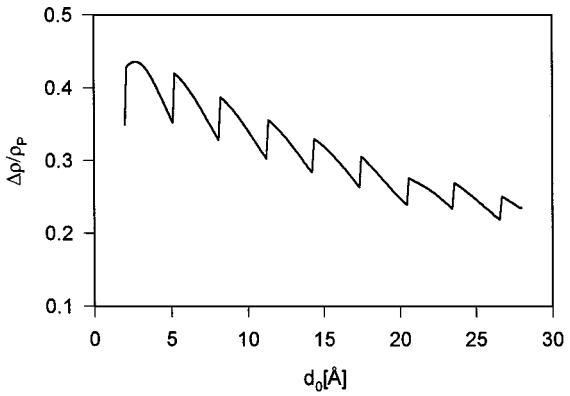

FIG. 4. Dependence of the GMR effect generated by the interfacial scattering potential on the spacer thickness for $d_1=d_2=20$ Å, $U_{1\pm}=U_{2\pm}=U_0=0$, $\tilde{V}_{1+}=\tilde{V}_{2+}=0$, $\tilde{V}_{1-}=\tilde{V}_{2-}=2$ eV, $\mu=4$ eV, $\lambda_{1\pm}=\lambda_{2\pm}=\lambda_0=400$ Å, $\eta_1=\eta_2=2$ Å, and $\xi_1=\xi_2=2$ Å.

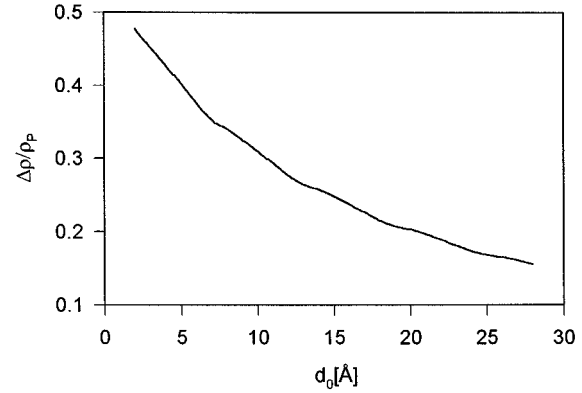

FIG. 5. GMR effect as a function of the spacer thickness d_0 calculated for $d_1=d_2=20$ Å, $U_{1\pm}=U_{2\pm}=1$ eV, $U_0=0$, $\mu=4$ eV, $\lambda_{1-}=\lambda_{2-}=200$ Å, $\lambda_{1+}=\lambda_{2+}=800$ Å, $\lambda_0=400$ Å, and $\eta_1=\eta_2=0$.

The situation changes when the interfaces are not flat and contribute to the electrical resistance. Consider the limit of vanishing potentials $\tilde{V}_{1\pm}$ and $\tilde{V}_{2\pm}$. The magnetoresistance originates then from the spin-dependent bulk scattering. However, the presence of interface roughness leads to additional oscillations in the resistivities and, consequently, to oscillations in the dependence of the magnetoresistance on the spacer thickness, as shown in Fig. 6 for two different values of the quantum well depth. The amplitude of the oscillations as well as the oscillation period is related to the depth of the quantum well in the spacer.

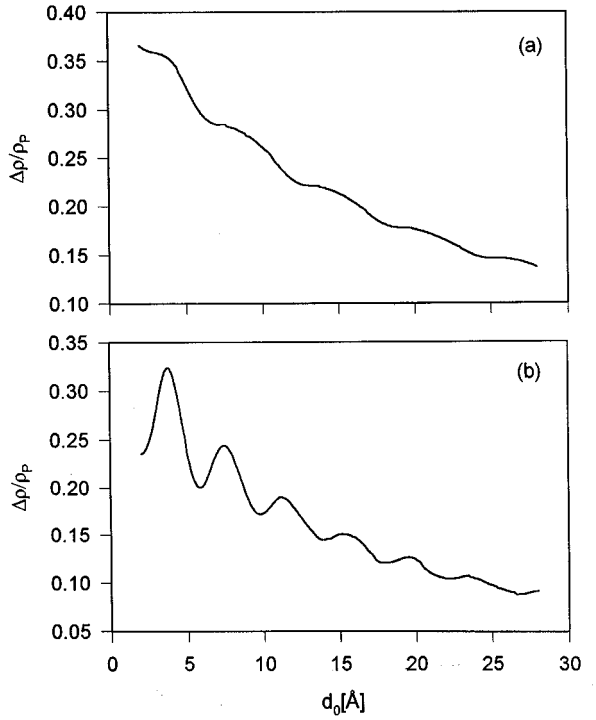

FIG. 6. GMR as a function of the spacer thickness d_0 calculated for $d_1=d_2=20$ Å, $\lambda_{1-}=\lambda_{2-}=200$ Å, $\lambda_{1+}=\lambda_{2+}=800$ Å, $\lambda_0=400$ Å, $\eta_1=\eta_2=2$ Å, $\xi_1=\xi_2=2$ Å, $\mu=4$ eV, $U_0=0$, and $\tilde{V}_{1\pm}=\tilde{V}_{2\pm}=0$. The other parameters are $U_{1\pm}=U_{2\pm}=1$ eV (a) and $U_{1\pm}=U_{2\pm}=2$ eV (b).

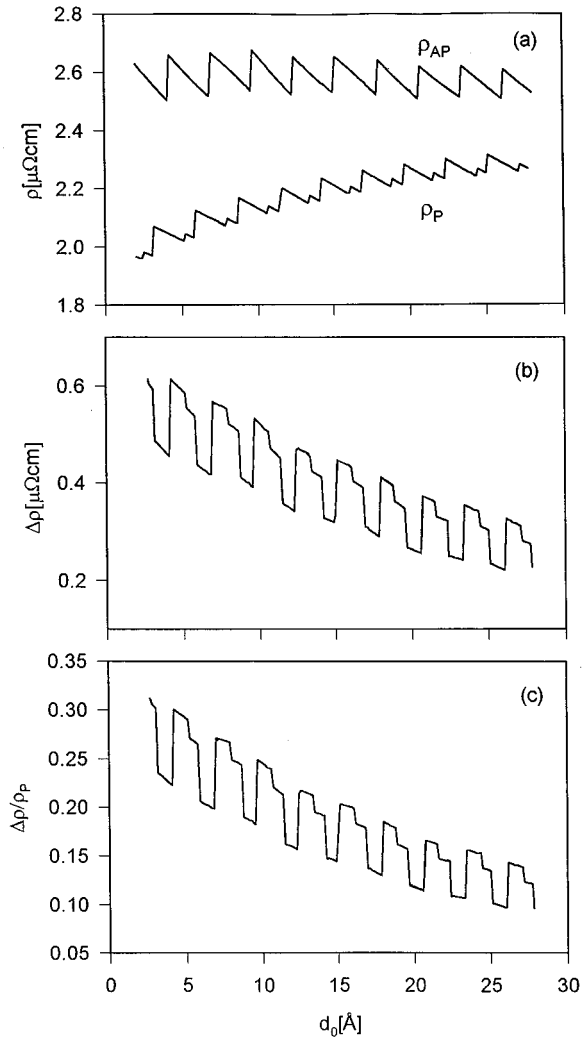

FIG. 7. (a) Electrical resistivities ρ_P and ρ_{AP}, (b) the resistance change, and (c) the GMR effect as a function of the spacer thickness d_0, calculated for $d_1=d_2=20$ Å, $\lambda_{1-}=\lambda_{2-}=200$ Å, $\lambda_{1+}=\lambda_{2+}=800$ Å, $\lambda_0=400$ Å, $\eta_1=\eta_2=0$, $\mu=5$ eV, $U_{1+}=U_{2+}=U_0=0$, and $U_{1-}=U_{2-}=0.5$ eV.

C. Spin-dependent quantum well in the spacer

Consider now the situation when the effective electron potential inside the ferromagnetic films depends on the electron spin orientation, giving rise to spin-dependent electron confinement inside the spacer (or ferromagnetic films).[15,30–32] Assume first the case of no interface roughness. The dependence of the resistivity, resistivity change, and the GMR effect on the spacer thickness is shown in Fig. 7. For parallel alignment of the film magnetizations, there is a phase shift between the oscillations in the contributions from the two spin channels, which results in a double-peak structure in the dependence of ρ_P on d_0. The phase shift is a consequence of the spin-dependent miniband structure for parallel configuration. For the antiparallel orientation the miniband structure is independent of the electron spin orientation (the structure assumed is symmetrical), and consequently there is no phase shift between the contributions from both spin channels. Another consequence of the spin-dependent miniband structure is a phase shift between the

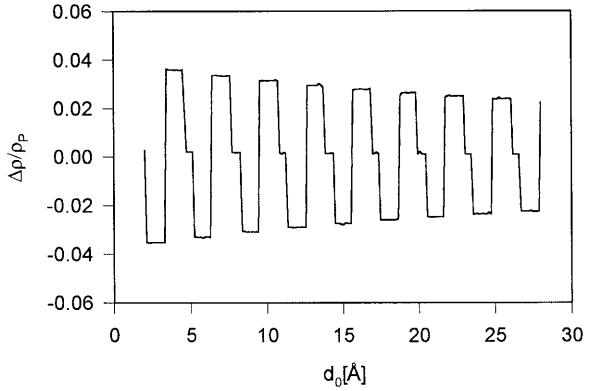

FIG. 8. GMR effect as a function of the spacer thickness, calculated for $d_1=d_2=20$ Å, $\lambda_{1\pm}=\lambda_{2\pm}=\lambda_0=400$ Å, $\mu=4$ eV, $U_{1+}=U_{2+}=U_0=0$, $U_{1-}=U_{2-}=0.5$ eV, and $\eta_1=\eta_2=0$.

oscillations in ρ_P and ρ_{AP}, which gives rise to the peculiar shape of the oscillations in $\Delta\rho$ [Fig. 7(b)]. This phase shift is also responsible for the oscillations in $\Delta\rho/\rho_P$ shown in Fig. 7(c). Oscillations similar to those shown in Fig. 7 also occur in the dependence of the resistivity, resistivity change, and GMR effect on the thickness of the magnetic films.

In Fig. 7 the magnetoresistance was due to the spin dependence of the bulk electron mean free paths in the magnetic films. It is interesting to note that the magnetoresistance, although small, still exists if there is no spin asymmetry in the electron mean free paths. Moreover, the magnetoresistance oscillates with the spacer thickness and the oscillations are associated with a change of the sign of the factor $\Delta\rho/\rho_P$, as shown in Fig. 8.

The interface roughness leads to effects which are similar to those discussed in Sec. IV B, i.e., to additional oscillations in resistivity and GMR.

D. Influence of the interface roughness

The interface roughness contributes to the GMR effect when the corresponding scattering potential depends on the electron spin orientation. This happens when either the electronic potential inside the magnetic films or the potential $\tilde{V}_{\beta\pm}$ is spin dependent. Assume first the limit of vanishing $\tilde{V}_{\beta\pm}$ for both interfaces. In Fig. 9 we show the GMR effect as a function of the roughness amplitude η ($\eta=\eta_1=\eta_2$) for several values of the correlation length ξ ($\xi=\xi_1=\xi_2$) and for no spin asymmetry in the bulk mean free paths. The GMR effect results now from the spin dependence of the interfacial scattering and increases with increasing amplitude of the roughness. It is also evident that the roughness with small correlation length ξ is more effective in generating the GMR effect than the roughness of the same amplitude but with a longer correlation length. A similar behavior of the magnetoresistance is observed when it is generated by the spin-dependent potentials $\tilde{V}_{\beta\pm}$, and the electronic potentials inside the magnetic films are independent of the electron spin.

In a general case, both bulk and interface spin-dependent scattering processes contribute to the GMR effect. Assume, for a while, perfect interfaces. The interface contribution to the resistivity and also to the GMR effect vanishes then exactly, and so the GMR is of bulk origin only. Consider now

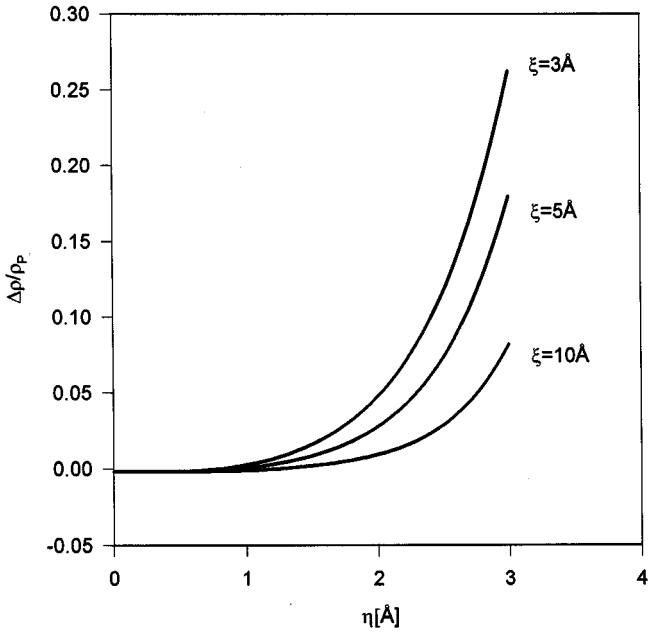

FIG. 9. GMR effect as a function of the roughness amplitude η for three values of the correlation length ξ. The other parameters assumed here are $d_1=d_2=20$ Å, $d_0=10$ Å, $U_{1-}=U_{2-}=1$ eV, $U_{1+}=U_{2+}=U_0=0$, $\tilde{V}_{1\pm}=\tilde{V}_{2\pm}=0$, $\mu=5$ eV, and $\lambda_{1\pm}=\lambda_{2\pm}=\lambda_0=500$ Å.

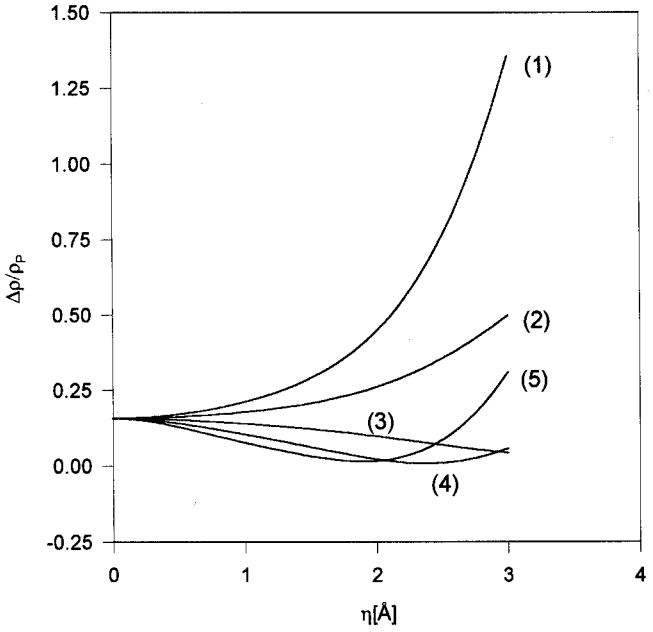

FIG. 10. GMR effect as a function of the roughness amplitude η for $d_1=d_2=20$ Å, $d_0=10$ Å. The other parameters assumed here are $d_1=d_2=20$ Å, $d_0=10$ Å, $U_{1\pm}=U_{2\pm}=U_0=0$, $\mu=5$ eV, $\lambda_{1+}=\lambda_{2+}=800$ Å, $\lambda_{1-}=\lambda_{2-}=200$ Å, $\lambda_0=100$ Å, and $\xi=3$ Å. Different curves correspond to the following values of $\tilde{V}_{\beta\pm}=\tilde{V}_{\pm}$ ($\beta=1,2$): (1) $\tilde{V}_+=0$, $\tilde{V}_-=2$ eV; (2) $\tilde{V}_{\pm}=0.5$ eV, $\tilde{V}_-=1.5$ eV; (3) $\tilde{V}_+=\tilde{V}_-=1.0$ eV; (4) $\tilde{V}_+=1.5$ eV, $\tilde{V}_-=0.5$ eV; (5) $\tilde{V}_+=2$ eV, $\tilde{V}_-=0$.

how a small interface roughness, with the corresponding scattering potential being spin dependent, can influence the GMR effect. What follows from numerical analysis is that a small roughness can either enhance or reduce the GMR effect generated by the bulk scattering. The enhancement takes place when the spin asymmetry for the interface and for bulk scattering is of the same kind: i.e., in both cases, the higher scattering rate is for electrons of the same spin orientation. If this is not the case, then the interface roughness reduces the GMR effect. This behavior is shown in Fig. 10, where $\Delta\rho/\rho_P$ is plotted as a function of the roughness amplitude. To eliminate the effects due to the spin-dependent electronic structure, a uniform electron potential across the structure was assumed, and so the interfaces contribute to the magnetoresistance only by the spin-dependent scattering potentials $\tilde{V}_{\beta\pm}$. For vanishing amplitude of the roughness, the effect is generated entirely by the bulk spin-dependent scattering. Different curves correspond to different spin asymmetries in the interfacial scattering potential. The curves denoted as (1) and (2) correspond to the situation when the minority electrons are scattered more effectively by the impurities as well as by the interface roughness. Consequently, the interface roughness enhances the GMR effect. Curve (3) corresponds to the interfacial scattering being independent of the spin orientation. The GMR effect decreases with increasing amplitude of the roughness because the relative role of the spin-dependent scattering decreases with increasing roughness. Curves (4) and (5), on the other hand, correspond to the case when the impurities scatter more effectively the minority electrons, whereas the interfaces scatter more strongly the majority electrons. The interface roughness compensates therefore a part of the GMR effect created by the scattering on impurities and reduces the effect. The GMR effect reaches a minimum at a point where both contributions almost cancel

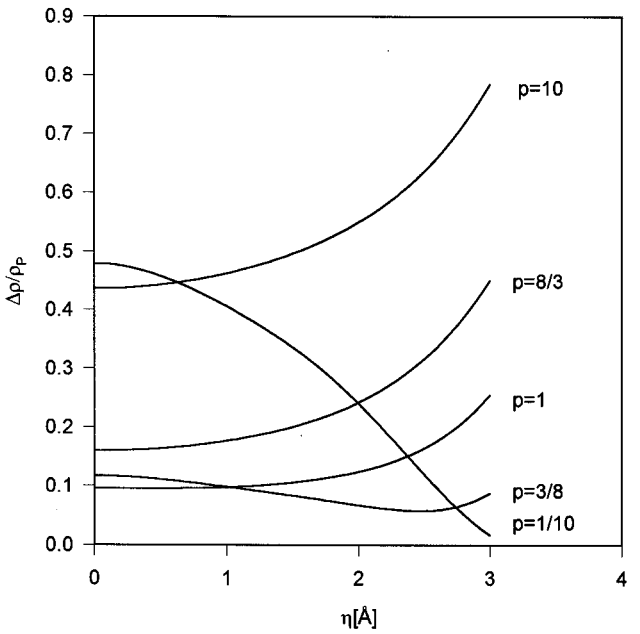

FIG. 11. GMR effect as a function of the roughness amplitude η for $d_1=d_2=20$ Å, $d_0=10$ Å, $U_{1-}=U_{2-}=1$ eV, $U_{1+}=U_{2+}=U_0=0$, $\tilde{V}_{1\pm}=\tilde{V}_{2\pm}=0$, $\mu=5$ eV, $\lambda_0=100$ Å, and $(\lambda_{1+}+\lambda_{1-})/2=(\lambda_{2+}+\lambda_{2-})/2=550$ Å with $p=\lambda_{1+}/\lambda_{1-}=\lambda_{2+}/\lambda_{2-}$ as indicated.

each other, and then the GMR increases again with a further increase of the roughness amplitude.

A similar behavior is shown in Fig. 11 in the limit of vanishing $\tilde{V}_{\beta\pm}$, when the interfacial scattering is entirely due to the spin-dependent potential steps $V_{\beta\pm}$. Different curves correspond to different values of the ratio p, $p=\lambda_{1+}/\lambda_{1-}=\lambda_{2+}/\lambda_{2-}$, with the average value of the electron mean free path being the same for both magnetic films, $(\lambda_{1+}+\lambda_{1-})/2=(\lambda_{2+}+\lambda_{2-})/2$, and also the same for all curves. For $p=10$ and $p=8/3$, the bulk and interface contributions to the GMR effect enhance each other. In the case of $p=3/8$ and $p=1/10$, the increasing roughness leads to a decrease of the GMR effect. The minimum seen for $p=3/8$ is of the same origin as the minima in Fig. 10.

V. SUMMARY

We analyzed the role of quantum size effects and interface roughness in the GMR effect in ultrathin magnetic sandwich structures. Within the one-band model with a parabolic electron band (which is additionally spin split in the ferromagnetic films), we showed that quantum size effects lead to oscillations in the dependence of the resistivity and GMR effect on the spacer thickness and also on the thickness of the magnetic films. The oscillation period is determined by the Fermi wavelength. If there is a quantum well in the spacer, then there is also an additional oscillation period which is related to the depth of the quantum well.

The interfacial roughness can generate the GMR effect in two different cases: (i) when the electronic potential in the magnetic films is spin dependent, which leads to spin-dependent potential steps at the interfaces, and (ii) when there are additional spin-dependent s-d scattering processes at the interfaces. If, however, there is also a contribution due to spin-dependent scattering on bulk defects, then the interface roughness can enhance or reduce the effect. The enhancement occurs when the spin asymmetry for the bulk scattering processes is of the same kind as that for the interface scattering. Long-range in-plane structural correlations in the interfacial roughness diminish its role in the GMR effect.

ACKNOWLEDGMENTS

We acknowledge financial support by the Belgian Interuniversity Attraction Poles (IUAP) and Flemish Concerted Action (GOA) programs. J.B. also acknowledges support through research Project No. 2 P 302 091 07 of the Polish Research Committee.

APPENDIX A

In this appendix we give the general formulas for the discrete energy levels $\epsilon_{\mu\sigma}$ and wave functions $\psi_{\mu\sigma}(z)$ introduced in Eqs. (10) and (11). In the following the spin index will be suppressed. For a given configuration of the sublayer magnetizations and for a given spin orientation, the problem reduces to solution of the Schrödinger equation for a spinless particle in a one-dimensional quantum well with infinite potential walls at $z=0$ and $z=L$, and with the steplike potential,

$$U(z)=\begin{cases} U_1, & 0\leq z\leq d_1, \\ U_0=0, & d_1<z\leq d_1+d_0, \\ U_2, & d_1+d_0<z\leq L, \end{cases} \tag{A1}$$

where U_1 and U_2 are constants and $U_1, U_2\geq 0$.

Applying the standard method, one finds the following dispersion equation for the discrete energy levels:

$$k_0^2 s_1 s_0 s_2 - k_0 k_2 s_1 c_0 c_2 - k_0 k_1 c_1 c_0 s_2 - k_1 k_2 c_1 s_0 c_2 = 0, \tag{A2}$$

where k_α ($\alpha=0,1,2$) is defined as $k_\alpha=[2m(U_\alpha-E)/\hbar^2]^{1/2}$ for $E<U_\alpha$ and $k_\alpha=[2m(E-U_\alpha)/\hbar^2]^{1/2}$ if $E>U_\alpha$. The other parameters in Eq. (A2) are defined as follows:

$$s_\alpha=\sinh(k_\alpha d_\alpha), \tag{A3a}$$

if $E<U_\alpha$, and

$$s_\alpha=\sin(k_\alpha d_\alpha), \tag{A3b}$$

when $E>U_\alpha$. Similarly,

$$c_\alpha=\cosh(k_\alpha d_\alpha), \tag{A4a}$$

if $E<U_\alpha$, and

$$c_\alpha=\cos(k_\alpha d_\alpha), \tag{A4b}$$

for $E>U_\alpha$.

Equation (A2) is fulfilled for some discrete values of the energy E, $E=\epsilon_\mu$, which are indexed in the following with μ, $\mu=1,2,3,\ldots$. The index μ will be also added to the corresponding parameters k_α, s_α, and c_α as well as to the appropriate wave functions.

The wave function $\psi_\mu(z)$ corresponding to the μth level is of the following form:

(i) For $0\leq z\leq d_1$,

$$\psi_\mu(z)=A_{1\mu}\sinh(k_{1\mu}z), \tag{A5a}$$

when $\epsilon_\mu<U_1$, and

$$\psi_\mu(z)=A_{1\mu}\sin(k_{1\mu}z), \tag{A5b}$$

if $\epsilon_\mu>U_1$.

(ii) For $d_1\leq z\leq d_1+d_0$,

$$\psi_\mu(z)=A_{0\mu}\sin[k_{0\mu}(z-d_1)]+B_{0\mu}\cos[k_{0\mu}(z-d_1)]. \tag{A6}$$

(iii) For $d_1+d_0\leq z\leq L$,

$$\psi_\mu(z)=A_{2\mu}\sinh[k_{2\mu}(z-L)], \tag{A7a}$$

when $\epsilon_\mu<U_2$, and

$$\psi_\mu(z)=A_{2\mu}\sin[k_{2\mu}(z-L)], \tag{A7b}$$

for $\epsilon_\mu>U_2$.

The constants $A_{1\mu}$, $A_{0\mu}$, $B_{0\mu}$, and $A_{2\mu}$ can be determined from the following set of equations:

$$A_{1\mu}s_{1\mu}=B_{0\mu}, \tag{A8a}$$

$$A_{0\mu}s_{0\mu}+B_{0\mu}c_{0\mu}=-A_{2\mu}s_{2\mu}, \tag{A8b}$$

$$A_{1\mu}k_{1\mu}c_{1\mu}=A_{0\mu}k_{0\mu}, \tag{A8c}$$

$$A_{0\mu}k_{0\mu}c_{0\mu}-B_{0\mu}k_{0\mu}s_{0\mu}=A_{2\mu}k_{2\mu}c_{2\mu}, \tag{A8d}$$

$$f_{1\mu}A_{1\mu}^2+f_{2\mu}A_{2\mu}^2+f_{0\mu}A_{0\mu}^2+f'_{0\mu}B_{0\mu}^2+2\,f''_{0\mu}A_{0\mu}B_{0\mu}=1. \tag{A8e}$$

The following definitions have been introduced here:

$$f_{1\mu}=\pm\left(\frac{1}{2}\,d_1-\frac{1}{2k_{1\mu}}\,s_{1\mu}c_{1\mu}\right), \tag{A9a}$$

$$f_{2\mu}=\pm\left(\frac{1}{2}\,d_2-\frac{1}{2k_{2\mu}}\,s_{2\mu}c_{2\mu}\right), \tag{A9b}$$

$$f_{0\mu}=\left(\frac{1}{2}\,d_0-\frac{1}{2k_{0\mu}}\,s_{0\mu}c_{0\mu}\right), \tag{A9c}$$

$$f'_{0\mu}=\left(\frac{1}{2}\,d_0+\frac{1}{2k_{0\mu}}\,s_{0\mu}c_{0\mu}\right), \tag{A9d}$$

$$f''_{0\mu}=\frac{1}{2k_{0\mu}}\,s_{0\mu}^2, \tag{A9e}$$

where the upper and lower signs in Eq. (A9a) [and Eq. (9b)] correspond, respectively, to $\epsilon_\mu>U_1$ and $\epsilon_\mu<U_1$ [$\epsilon_\mu>U_2$ and $\epsilon_\mu<U_2$].

APPENDIX B

Here we present the explicit expressions for $K_{\alpha\sigma}^{\nu\mu}$ defined by Eq. (26) (the spin index is suppressed also in this appendix). Taking into account the explicit forms of the states $\psi_\mu(z)$ (Appendix A), one finds

$$K_1^{\nu\mu}=\frac{1}{8}\,\delta A_{1\nu}^2A_{1\mu}^2\left[\frac{k_{1\mu}C_{1\nu}S_{1\mu}-\delta k_{1\nu}S_{1\nu}C_{1\mu}}{(k_{1\mu})^2-\delta(k_{1\nu})^2}-\frac{S_{1\mu}}{k_{1\mu}}-\frac{S_{1\nu}}{k_{1\nu}}+2d_1\right], \tag{B1a}$$

for $\nu\neq\mu$, and

$$K_1^{\nu\nu}=\frac{1}{8}\,A_{1\nu}^4\left(\frac{S_{1\nu}C_{1\nu}}{2k_{1\nu}}-2\,\frac{S_{1\nu}}{k_{1\nu}}+3d_1\right), \tag{B1b}$$

if $\nu=\mu$. Here $\delta=-1$ if only one of the levels ϵ_ν and ϵ_μ is lower than U_1 and $\delta=1$ otherwise, whereas $S_{1\mu}$ and $C_{1\mu}$ are defined as follows:

$$S_{1\mu}=\sinh(2k_{1\mu}d_1), \tag{B2a}$$

$$C_{1\mu}=\cosh(2k_{1\mu}d_1), \tag{B2b}$$

when $\epsilon_\mu<U_1$, and

$$S_{1\mu}=\sin(2k_{1\mu}d_1), \tag{B2c}$$

$$C_{1\mu}=\cos(2k_{1\mu}d_1), \tag{B2d}$$

when $\epsilon_\mu>U_1$. The amplitudes $A_{1\nu}$ and $A_{1\mu}$ are given by the solutions of Eqs. (A8a)–(A8e).

Similar formulas hold also for $K_2^{\nu\mu}$. They can be obtained from the above formulas (B1a)–(B2d) by replacing everywhere the index 1 by the index 2. Finally, $K_0^{\nu\mu}$ is given by

$$\begin{aligned}K_0^{\nu\mu}=\frac{1}{16}\Bigg[&[(A_{0\nu}^2-B_{0\nu}^2)(A_{0\mu}^2-B_{0\mu}^2)-4A_{0\nu}B_{0\nu}A_{0\mu}B_{0\mu}]\,\frac{\sin[2(k_{0\nu}+k_{0\mu})d_0]}{k_{0\nu}+k_{0\mu}}+[(A_{0\nu}^2-B_{0\nu}^2)(A_{0\mu}^2-B_{0\mu}^2)\\&+4A_{0\nu}B_{0\nu}A_{0\mu}B_{0\mu}]\,\frac{\sin[2(k_{0\nu}-k_{0\mu})d_0]}{k_{0\nu}-k_{0\mu}}-2(A_{0\nu}^2-B_{0\nu}^2)(A_{0\mu}^2+B_{0\mu}^2)\,\frac{\sin(2k_{0\nu}d_0)}{k_{0\nu}}-2(A_{0\nu}^2+B_{0\nu}^2)(A_{0\mu}^2\\&-B_{0\mu}^2)\,\frac{\sin(2k_{0\mu}d_0)}{k_{0\mu}}+4(A_{0\nu}B_{0\mu}+B_{0\nu}A_{0\mu})(B_{0\nu}B_{0\mu}-A_{0\nu}A_{0\mu})\left(\frac{\sin^2[(k_{0\nu}+k_{0\mu})d_0]}{k_{0\nu}+k_{0\mu}}+\frac{\sin^2[(k_{0\nu}-k_{0\mu})d_0]}{k_{0\nu}-k_{0\mu}}\right)\\&+8A_{0\nu}B_{0\nu}(A_{0\mu}^2+B_{0\mu}^2)\,\frac{\sin^2(k_{0\nu}d_0)}{k_{0\nu}}+8(A_{0\nu}^2+B_{0\nu}^2)A_{0\mu}B_{0\mu}\,\frac{\sin^2(k_{0\mu}d_0)}{k_{0\mu}}+4d_0(A_{0\nu}^2+B_{0\nu}^2)(A_{0\mu}^2+B_{0\mu}^2)\Bigg],\end{aligned} \tag{B3a}$$

for $\nu\neq\mu$, and

$$\begin{aligned}K_0^{\nu\nu}=\frac{1}{16}\Bigg[&(A_{0\nu}^4+B_{0\nu}^4-6A_{0\nu}^2B_{0\nu}^2)\,\frac{\sin(4k_{0\nu}d_0)}{2k_{0\nu}}+4(B_{0\nu}^4-A_{0\nu}^4)\,\frac{\sin(2k_{0\nu}d_0)}{k_{0\nu}}+6d_0(A_{0\nu}^2+B_{0\nu}^2)^2\Bigg]+\frac{1}{k_{0\nu}}\,[A_{0\nu}^3B_{0\nu}\sin^4(k_{0\nu}d_0)\\&+A_{0\nu}B_{0\nu}^3[1-\cos^4(k_{0\nu}d_0)]],\end{aligned} \tag{B3b}$$

for $\nu=\mu$.

*Permanent address: Magnetism Theory Division, Institute of Physics, A. M. University, ul. Matejki 48/49, 60-769 Poznań, Poland.

[1] M. N. Baibich, J. M. Broto, A. Fert, F. Nguyen van Dau, F. Petroff, P. Etienne, G. Creuzet, A. Friederich, and J. Chazelas, Phys. Rev. Lett. **61**, 2472 (1988).

[2] G. Binasch, P. Grünberg, F. Saurenbach, and W. Zinn, Phys. Rev. B **39**, 4828 (1989).

[3] For a review, see S. S. P. Parkin, in *Ultrathin Magnetic Structures II*, edited by B. Heinrich and J. A. C. Bland (Springer-Verlag, Berlin, 1994), p. 148.

[4] J. Barnaś, A. Fuss, R. E. Camley, P. Grünberg, and W. Zinn, Phys. Rev. B **42**, 8110 (1990); J. Barnaś, A. Fuss, R. E. Camley, U. Walz, P. Grünberg, and W. Zinn, Vacuum **41**, 1243 (1990).

[5] J. M. George, L. G. Pereira, A. Barthelemy, F. Petroff, L. Steren, J. L. Duvail, A. Fert, R. Loloee, P. Holody, and P. A. Schroeder,

Phys. Rev. Lett. **72**, 408 (1994).
[6] R. Schad, C. D. Potter, P. Belien, G. Verbanck, V. V. Moshchalkov, and Y. Bruynseraede, Appl. Phys. Lett. **64**, 3500 (1994).
[7] H. Kano, K. Kagawa, A. Suzuki, A. Okabe, K. Hagashi, and K. Aso, Appl. Phys. Lett. **63**, 2839 (1993).
[8] R. E. Camley and J. Barnaś, Phys. Rev. Lett. **63**, 664 (1989).
[9] P. M. Levy, S. Zhang, and A. Fert, Phys. Rev. Lett. **65**, 1643 (1990); S. Zhang, P. M. Levy, and A. Fert, Phys. Rev. B **45**, 8689 (1992).
[10] J. L. Duvail, A. Fert, L. G. Pereira, and D. K. Lottis, J. Appl. Phys. **75**, 7070 (1994).
[11] K. M. Schep, P. J. Kelly, and G. E. W. Bauer, Phys. Rev. Lett. **74**, 586 (1995).
[12] B. Dieny, J. Phys. Condens. Matter **4**, 8009 (1992); Europhys. Lett. **17**, 261 (1992).
[13] A. Barthelemy and A. Fert, Phys. Rev. B **43**, 13124 (1991).
[14] R. Q. Hood and L. M. Falicov, Phys. Rev. B **46**, 8287 (1992); R. Q. Hood, L. M. Falicov, and D. R. Penn, *ibid*. **49**, 368 (1994).
[15] A. Vedyayev, B. Dieny, and N. Ryzhanova, Europhys. Lett. **19**, 329 (1992); A. Vedyayev, C. Cowache, N. Ryzhanova, and B. Dieny, J. Phys. Condens. Matter **5**, 8289 (1993).
[16] H. E. Camblong and P. M. Levy, Phys. Rev. Lett. **69**, 2835 (1992).
[17] J. Barnaś and A. Fert, Phys. Scr. T **49**, 264 (1993); J. Barnaś, J. Magn. Magn. Mater. **131**, L14 (1994).
[18] B. Bulka and J. Barnaś, Phys. Rev. B **51**, 6348 (1995).
[19] H. Hasegawa, Phys. Rev. B **47**, 15 073 (1993); **47**, 15 080 (1993).
[20] Y. Asano, A. Oguri, and S. Maekawa, Phys. Rev. B **48**, 6192 (1993).
[21] H. Itoh, J. Inoue, and S. Maekawa, Phys. Rev. B **51**, 342 (1995).
[22] N. Trivedi and N. W. Ashcroft, Phys. Rev. B **38**, 12 298 (1988).
[23] D. Calecki, Phys. Rev. Lett. **62**, 1302 (1989); Phys. Rev. B **43**, 11 581 (1991).
[24] E. E. Fullerton, D. M. Kelly, J. Guimpel I. K. Schuller, and Y. Bruynseraede, Phys. Rev. Lett. **68**, 859 (1992).
[25] F. Petroff, A. Barthelemy, A. Fert, P. Etienne, and S. Lequien, J. Magn. Magn. Mater. **93**, 95 (1991).
[26] Y. Obi, K. Takanashi, Y. Mitami, N. Tsuda, and H. Fujimori, J. Magn. Magn. Mater. **104–107**, 1747 (1992).
[27] P. Belien, R. Schad, C. D. Potter, G. Verbanck, V. V. Moshchalkov, and Y. Bruynseraede, Phys. Rev. B **50**, 9957 (1994).
[28] N. F. Mott, Adv. Phys. **13**, 325 (1964).
[29] Preliminary results were published as a Letter, J. Barnaś and Y. Bruynseraede, Europhys. Lett. **32**, 167 (1995).
[30] P. B. Visscher, Phys. Rev. B **49**, 3907 (1994).
[31] S. Zhang and P. M. Levy, in *Magnetic Ultrathin Films*, edited by B. T. Jonker, MRS Symposia Proceedings No. 313 (Materials Research Society, Pittsburgh, 1993), p. 53.
[32] A. C. Ehrlich, Phys. Rev. Lett. **71**, 2300 (1993).